Research article

Jie Li, Lin Du, Jing Huang, Yuan He, Jun Yi, Lili Miao*, Chujun Zhao and Shuangchun Wen

Passive photonic diodes based on natural van der Waals heterostructures

https://doi.org/10.1515/nanoph-2020-0442
Received August 3, 2020; accepted October 25, 2020;
published online November 9, 2020

Abstract: Van der Waals heterostructures are composed of stacked atomically thin two-dimensional (2D) crystals to provide unprecedented functionalities and novel physics. Franckeite, a naturally occurring van der Waals heterostructure consisting of superimposed SnS_2-like and PbS-like layers alternately, shows intriguing potential in versatile optoelectronic applications. Here, we have prepared the few-layer franckeite via liquid-phase exfoliation method and characterized its third-order nonlinearity and ultrafast dynamics experimentally. We have found that the layered franckeite shows low saturable intensity, large modulation depth and picosecond ultrafast response. We have designed the passive photonic diodes based on the layered franckeite/C_{60} cascaded film and suspension configuration and found that the passive photonic diodes exhibit stable nonreciprocal transmission of light. The experimental results show the excellent nonlinear optical performance and ultrafast response of the layered franckeite, which may make inroad for the cost effective and reliable high-performance optoelectronic devices.

***Corresponding author: Lili Miao**, Key Laboratory for Micro/Nano Optoelectronic Devices of Ministry of Education & Hunan Provincial Key Laboratory of Low-Dimensional Structural Physics and Devices, School of Physics and Electronics, Hunan University, Changsha 410082, China, E-mail: lilimiao@hnu.edu.cn. https://orcid.org/0000-0001-7514-8374

Jie Li, Lin Du, Jing Huang, Yuan He, Jun Yi, Chujun Zhao and Shuangchun Wen, Key Laboratory for Micro/Nano Optoelectronic Devices of Ministry of Education & Hunan Provincial Key Laboratory of Low-Dimensional Structural Physics and Devices, School of Physics and Electronics, Hunan University, Changsha 410082, China, E-mail: jiezai@hnu.edu.cn (J. Li), lindu@hnu.edu.cn (L. Du), huangjing_2018hnu@163.com (J. Huang), yuanhe@hnu.edu.cn (Y. He), junyi@hnu.edu.cn (J. Yi), cjzhao@hnu.edu.cn (C. Zhao), scwen@hnu.edu.cn (S. Wen). https://orcid.org/0000-0002-7924-9524 (C. Zhao)

Keywords: franckeite; nonlinear optics; photonic diode; spatial self-phase modulation; ultrafast carrier dynamics; Z-scan.

1 Introduction

Van der Waals heterostructures (vdWHs) [1–3], composed of stacked atomically thin two-dimensional (2D) crystals, exhibit unprecedented physicochemical properties for exploring new physical or chemical phenomena and intriguing applications ranging from solar cell [4, 5], catalysis [6, 7] to artificial intelligence devices [8, 9]. Bandgap and structure engineering of vdWHs can bring novel functionalities for the optical, electrical, and optoelectronic devices, like modulators [10, 11], tunneling transistors [12], filters [13], and light-emitting diodes [14]. Recently, the fabrication of superlattices based on 2D materials through vertical stacking, atomic or molecular embedding, moiré patterning, strain engineering, and lithography has become a strategy to explore new quantum phenomena and further tune the performance of optoelectronic devices [15–17]. However, vdWHs are usually obtained via mechanical exfoliation and manual restacking process, which is uncertain and challenging due to the need of controlling the crystal arrangement of different crystal lattices and avoiding the introduction of interlayer adsorbates [18]. Franckeite, a naturally occurring heterostructure with superimposed SnS_2-like and PbS-like layers alternately, was found by Velický et al. [19] and Molina-Mendoza et al. [20] in 2017. But even more important, the franckeite is a stable 2D semiconductor with *p*-type doping and narrow bandgap (<0.7 eV) [20, 21]. The spontaneous rippling shows that franckeite breaks the initial lattice symmetry of a single layer and shows structurally anisotropy [22]. All the physicochemical characteristics make franckeite an excellent candidate for high-performance optoelectronic devices [23–25].

With the development of all-optical networks, all-optical signal processing without passing into the electrical domain becomes more and more important for high-speed and cost-effective characteristics [26]. Photonic

Open Access. © 2020 Jie Li et al., published by De Gruyter. This work is licensed under the Creative Commons Attribution 4.0 International License.

diode can realize the one-way transmission of light to prevent the backward transmitted light from causing adverse effects on the light source and the optical path system, which can be used in the fields of optical computing, optical interconnection, laser and so on. To date, different mechanisms and methods such as photonic crystals [27, 28], magneto-optical effects [29], liquid crystal heterojunctions [30] and nonlinear optical effects [31–34] have been proposed to achieve unidirectional light transmission. With the development of low-dimensional (LD) materials, their broadband optical response, tunable absorption, compact structure and ease of preparation provide the possibility for novel all-optical information processing devices [35–37].

Here, we prepared the layered franckeite by liquid-phase exfoliation (LPE) method. The saturable absorption (SA) characteristics of franckeite were studied through the open aperture (OA) Z-scan experiment, and the nonlinear absorption coefficient of about -1.95×10^{-4} m/W, saturable intensity of 0.18 kW/cm^2, and modulation depth of 9.4% were obtained at 1064 nm wavelength. This relatively low-threshold saturable intensity and large modulation depth makes photonic diodes more easily implemented. Ultrafast carrier dynamics characteristic with hundred picoseconds makes franckeite have the potential to contribute to the ultrafast optoelectronic devices. Based on the optical Kerr effect of franckeite, the spatial self-phase modulation (SSPM) effect was measured during the interaction of light-franckeite and the formation of a diffraction ring was observed clearly. Combining with the optical limiting (OL) characteristics of C_{60}, a franckeite/C_{60}-based photonic diode was designed based on the nonlinear optical properties of franckeite to realize nonreciprocal transmission of light, and the nonreciprocity factor was about 2 dB obtained experimentally. Further research found that the nonreciprocal characteristics of the passive photonic diode can be tuned by adjusting the nonlinear parameters, and the SA with low-threshold saturable intensity and large modulation depth can provide more possibilities for the passive photonic diodes.

2 Characterization of layered franckeite

The layered franckeite was prepared from its bulk form by LPE method [21, 38]. The franckeite-NMP (*N*-methyl-2-pyrrolidone) dispersion was suspended on a 1-mm quartz glass plate to prepare a thin film. Scanning electron microscope (SEM) and transmission electron microscopy (TEM) were employed to characterize the morphology. The SEM image in Figure 1A shows that the bulk franckeite has been stripped into flakes. The TEM and corresponding atomic scale high-resolution TEM were also characterized in Figure 1B and C, showing that the observed interdistances of the lattice fringes were found to be 0.33 nm ((100), SnS_2-like) and 0.298 nm ((020), PbS-like). Figure 1D, E, and F show the morphology and thickness information of the layered franckeite film conducted by the atomic force microscopy (AFM) measurement. For precisely analyzing the thickness of franckeite flakes, four different sections were chosen for the measurements, as marked A, B, C, and D in Figure 1D. Figure 1E shows the height difference between the substrate and target sections. The thicknesses of the section A to section D are measured to be about 20.5, 11.3, 7.8 and 6.4 nm, respectively. The statistical analysis of the original height data of AFM shows that the nanoflakes from ~3 layers (3L) to ~6L are more widely distributed in the franckeite film (unit cell, H + Q layer, thickness 1.7 nm [20]), as shown in Figure 1F. Raman spectroscopy can clearly show the presence of PbS-like and SnS_2-like compounds, as shown in Figure 1G. The intense, strong peak at about 69 cm^{-1} corresponds to the acoustic mode of PbS-like [39, 40], and the peak at 315 cm^{-1} corresponds to the A_{1g} mode of SnS_2-like [41, 42]. Other peaks at 122, 190, 253, and the 400–600 cm^{-1} shoulder are roughly due to the superposition of respective phonon modes of both PbS (including longitudinal optical [LO], 2LO, 3LO modes) and SnS_2 (including the E_g mode and 2nd order effects) [42–44 [42–44]]. The linear transmittance spectrum shows the broadband absorption characteristic of franckeite, which verifies its narrow bandgap energy (<0.7 eV) [20, 21]. It is worth noting that the transmission spectrum shows a small valley around 1.1 μm wavelength, which is likely related to the superlattice plasma effect introduced by the moiré fringes [24]. Here, we have carried out further research on nonlinear absorption characteristics in the near infrared region to explore its application potential in optoelectronic devices.

3 Third-order nonlinear optical characteristics and ultrafast response of franckeite

The OA Z-scan was used to investigate the nonlinear optical characteristics of franckeite [45, 46], and the prepared franckeite film was used as the sample. We employed the mode-locked pulse laser with the central wavelength

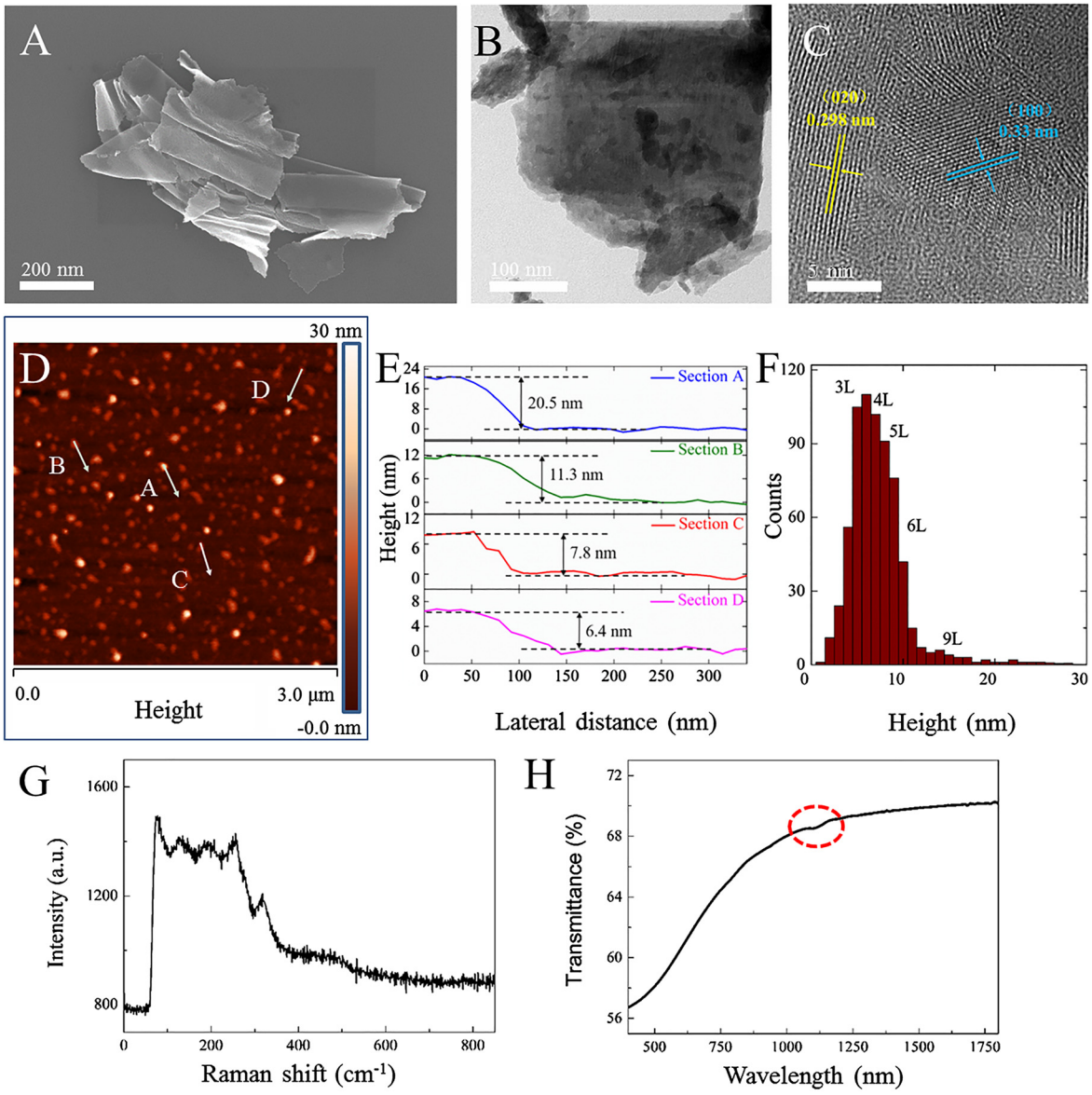

Figure 1: Material characteristics of the layered franckeite.
(A) Scanning electron microscope (SEM) micrograph of layered franckeite after liquid-phase exfoliation (LPE). (B) transmission electron microscopy (TEM) image of layered franckeite. (C) The corresponding atomic scale high-resolution TEM (HRTEM) of an ultrathin franckeite layer. (D) Two-dimensional topographical atomic force microscopy (AFM) image of franckeite film. (E) Height profiles of the sections marked in Figure 1D. (F) Statistical analysis of the AFM raw height data. The inserted numbers prove that the nanoflakes from ~3 layers (3L) to ~6L are more widely distributed (unit cell, H + Q layer, thickness 1.7 nm [20]). (G) Raman spectra of layered franckeite. (H) The linear transmittance of layered franckeite shows a small valley around 1.1 μm wavelength.

1064 nm, pulse duration 220 ps, repetition rate 2.8 MHz. Typical OA Z-scan curves are shown in Figure 2A and C. Figure 2B and D are the absorption characteristic curves obtained from the change of z into the change of light intensity. The Z-scan curve of franckeite shows a peak trend and is symmetrical about the laser focus, indicating that the absorption of the material decreases with the increasing light intensity. However, when the transmittance gradually becomes gentle with the increasing light intensity, it indicates that the absorption reaches saturation, which proves that franckeite has SA characteristics. Conversely, the Z-scan curve of C_{60} is symmetrical about the laser focus and shows a valley trend, that is, the absorption of the material increases with the increasing light intensity (reverse saturable absorption [RSA]), indicating the potential of C_{60} as an OL material.

The optical transmittance of OA Z-scan trace can be fitted by the formula:

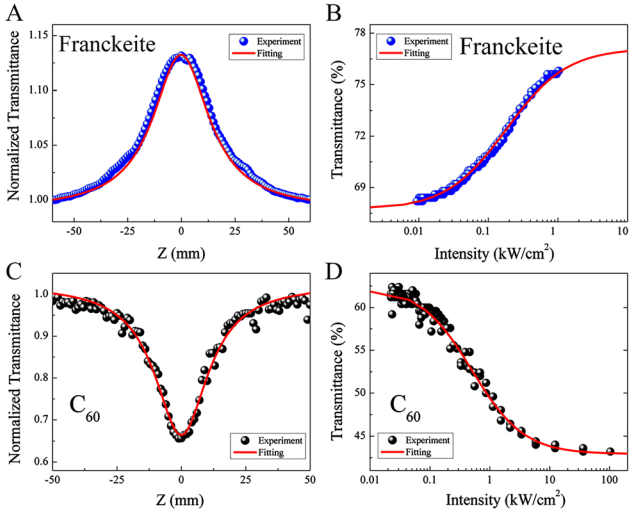

Figure 2: Nonlinear optical characteristics of layered franckeite and C_{60}.
Open aperture (OA) Z-scan curves of (A) franckeite and (C) C_{60} at 1064 nm wavelength, respectively. The corresponding relationship between transmittance and input intensity of (B) franckeite and (D) C_{60}, respectively.

$$T_{(z)} = 1 - \frac{\beta I_0 L_{\text{eff}}}{2\sqrt{2}(1 + z^2/z_0^2)} \tag{1}$$

β is the nonlinear absorption coefficient, and I_0 means the focal light intensity of the incident laser. The effective length $L_{\text{eff}} = \frac{[1-e^{-\alpha_0 L}]}{\alpha_0}$ of sample can be obtained by substituting the sample length L and linear absorption coefficient α_0. $z_0 = \frac{k\omega_0^2}{\lambda}$ is the diffraction length of the beam, and the waist radius ω_0 of beam focus is about 60 μm measured by the knife edge method.

The relationship between the optical transmittance and the optical intensity can be fitted by the formula:

$$T_{(I)} = 1 - \left(\frac{\alpha_s}{1 + I/I_s} + \alpha_{ns}\right) \tag{2}$$

α_s means the saturable loss or modulation depth and α_{ns} is the nonsaturable loss, I_s is the saturable optical intensity (for SA) or limiting threshold (for RSA).

By fitting the experimental data, we obtained the SA characteristics of franckeite: the value of the nonlinear absorption coefficient is about -1.95×10^{-4} m/W, the saturable optical intensity ~0.18 kW/cm^2, and the modulation depth of 9.4%. The SA response of franckeite with low-threshold SA and large modulation depth may provide novel nonlinear optical application in near infrared spectral range. Meanwhile, the C_{60} exhibits excellent OL characteristics with a limiting threshold ~0.498 kW/cm^2 and a modulation depth of 9.8%.

Femtosecond transient absorption spectroscopy has the advantages of high time resolution and wide measurement range, which is an effective tool for studying ultrafast dynamic processes of organic or inorganic materials. In the measurement of femtosecond transient absorption spectroscopy, a strong 400 nm wavelength laser is used as the pump light, which is focused into the sample after proper attenuation and polarization direction adjustment. The weaker laser is focused into the nonlinear crystal to generate supercontinuum white light as the signal light and adjusted by the time delay device then focused to the same position of the sample. The time delay device is used to adjust the optical path difference between pump and signal lights, the modulation signal is achieved by white light passing through the sample under different time delays and collected by the line photodiode.

Figure 3 shows the change in optical density of signal light of different wavelengths within a certain delay time after the material is excited, and the positive signal indicates that RSA occurs while the negative signal indicates that SA occurs. The results show that franckeite make a broadband absorption in visible range, especially the ultrafast carrier dynamic processes (about 50–800 ps) generated near ~500 nm wavelength, which means the complex and competitive absorption process occurs (may including SA caused by ground state bleaching, RSA signal caused by excited state absorption, etc.). Ultrafast carrier dynamics characteristic makes franckeite have the potential to an excellent candidate for ultrafast optoelectronic devices.

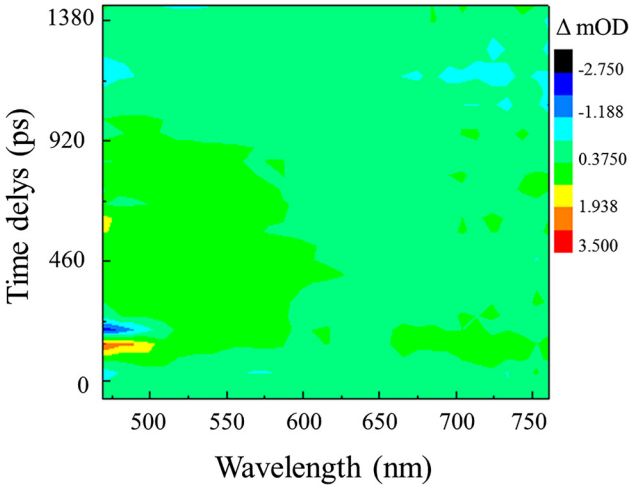

Figure 3: Transient absorption spectroscopy of franckeite. It can be seen that the franckeite make a broadband absorption, especially the multiple ultrafast signals (about 50–800 ps, as shown in the yellow, blue, and green regions) generated near 500 nm wavelength. Color bars indicate changes in optical density.

4 Passive photonic diodes based on nonlinear optical characteristics of franckeite

The nonlinear optical properties of LD materials can be used in photonic applications, such as optical modulators [47, 48], isolators [31], and switchers [49] for signal processing, mode-locked lasers for generating ultrashort pulses [50]. By cascading two materials with opposite nonlinear optical behavior in light path, namely introducing nonlinear discontinuities, the axial asymmetry function of the photodiode can be realized. The passive photonic diode was obtained by stacking the franckeite and C_{60} to achieve the nonreciprocal transmission of light.

In the passive photonic diode structure (as shown in Figure 4), the laser in forward bias passes through SA-RSA films in turn with an overall transmittance increases due to the enhanced transmitted beam of nonlinear part (dark red), which is equivalent to the light-conducting function of the optical diode. Conversely, the total transmittance of the light after passing through the RSA-SA films is reduced in the reverse bias setting, which means the light cutoff function is realized.

For an SA nonlinear material, the intensity absorption coefficient is given by [51]:

$$\alpha_{SA}(I) = \frac{\alpha_{0SA}}{(1 + I/I_s)} \tag{3}$$

The generalized pulse propagation equation is obtained as

$$\frac{dI}{dz'} = -\frac{\alpha_{0SA}}{1 + I/I_s} \times I \tag{4}$$

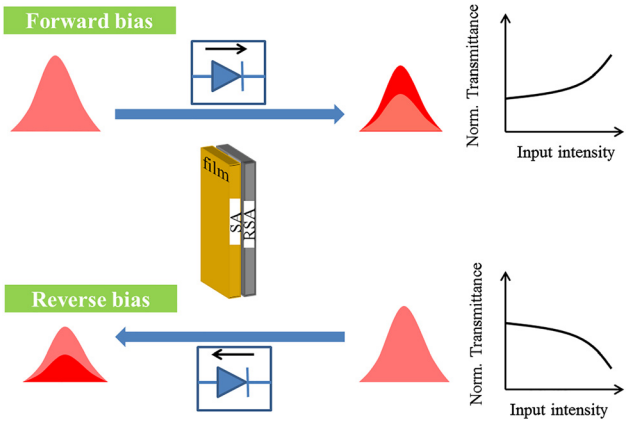

Figure 4: Action of an all-optical diode based on asymmetric nonlinear absorption. Dark red represents nonlinear transmission, light red represents linear transmission.

where z' is the position coordinate along the axis of propagation in the medium (of length L) and I is $I(z', t)$.

For RSA material, $I \le I_s$, the nonlinear absorption coefficient can be given by:

$$\alpha_{RSA}(I) = \alpha_{0RSA} + \beta_{2PA} I^2 \tag{5}$$

β_{2PA} is the two-photon absorption coefficient. The differential equation describing the optical loss of RSA is given by

$$\frac{dI}{dz'} = -\alpha_{0RSA} I - \beta_{2PA} I^2 \tag{6}$$

For the passive photonics diode, the nonreciprocity factor is defined as:

$$dB = 10 \times 1g\left(T_{forward}/T_{reverse}\right) \tag{7}$$

where $T_{forward}$ and $T_{reverse}$ are the nonlinear transmittance values for forward and reverse directions (as shown in Figure 4).

Based on the above theoretical model, combined with the third-order nonlinear optical characteristics of the two nonlinear optical materials, we theoretically and experimentally studied the nonreciprocal optical transmission of the passive photonic diode based on franckeite and C_{60}, as shown in Figure 5. Based on different values of I_s and α_s, we studied the influence of nonlinear parameters on the transmission characteristics of the photonic diode, as shown in Figure 5A and B. In both cases, the transmission is reciprocal when the input intensity is less than 0.1 kW/cm^2, but at a higher intensity, nonreciprocity is excited and realized to different degrees.

The performance of a nonlinear photonic diode is more affected by the characteristics of SA, the nonreciprocal factor gradually increases with the decrease of I_s or increase of α_s. The results show that SA materials with larger modulation depth and lower saturable intensity will have more potential to develop photonic diodes and even other optoelectronic devices. The prepared franckeite/C_{60} was placed in forward bias and reverse bias under the same condition, the passive all-optical diode with a nonreciprocity factor of about 2 dB was obtained experimentally (Figure 5D). Combined with ultrafast broadband nonlinear response of franckeite [21], the realization of the franckeite-based passive photonic diode will open up its application potential in photonic and optoelectronic fields in the near-infrared spectral range.

We also verified the photonic diode with the franckeite in solution to realize the nonreciprocal transmission of light [31, 33]. The refractive index of franckeite is modulated by the incident light intensity, the change in the refractive index induced by the light field will cause a

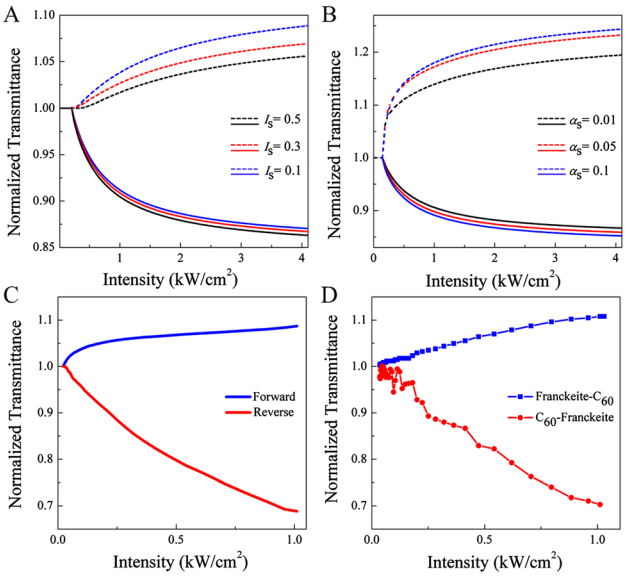

Figure 5: Nonreciprocal transmission characteristics of the passive photonic diode based on nonlinear optics.
(A) Different values of I_s. (B) Different values of α_s. Nonreciprocal transmission characteristics of the photonic diode based on franckeite/C_{60} obtained (C) theoretically and (D) experimentally. The nonreciprocity factor ~2 dB of the passive photonic diode was obtained.

phase change. That is, the phase of incident laser beam can be modulated by its own intensity when propagating in the nonlinear optical medium, which is known as self-phase modulation (SPM) [51]. The SSPM is an SPM generated on the cross section of the beam, which is used to develop the nonlinear optical characteristics of LD materials [52–54].

The nonlinear phase change $\Delta\varphi(r) \approx \Delta\varphi_0 \exp(-2r^2/\omega^2)$ shows Gaussian distribution along the radial direction r for a Gaussian beam, the light is strongest at the center of $r = 0$ which causes the largest $\Delta\varphi_0$. If $|\Delta\varphi_0|$ is much larger than 2π, then the center symmetrical peak or valley appears at equal r in the horizontal output power spectrum, thus the projection of the far field appears a ring structure of bright and dark intervals. This is the result of light interference between rings with the same dip angle and different radii (different phases). The number of bright and dark rings is close, and this number is close to the integer of $|\Delta\varphi_0|/\pi$. The diameter of the outermost ring is determined by the maximum slope of $\Delta\varphi(r)$ at the Gaussian pattern inflection point. In addition, the collapse of diffraction ring (Figure 6A) is mainly caused by the asymmetric thermal convection introduced by gravity during the action. The nonlinear refractive index n_2 of the natural vdWHs layered franckeite was calculated to be ~10^{-9} m^2/W at 1064 nm wavelength [21].

The significant nonlinear optical characteristics of layered franckeite make it have the potential to excite the diffraction rings, but the RSA characteristic of C_{60} make it have the effect of reducing the light intensity. In Figure 6, the franckeite and C_{60} dispersions were filled in two closely matched cuvettes to form a mixed structure, which was used as a nonlinear photonic diode to realize the nonreciprocal propagation of light. When the laser passes through the forward bias (franckeite-C_{60}), the diffraction ring will be excited when passing through franckeite dispersion then successively passing through C_{60}, that is to achieve the forward light conduction function (the

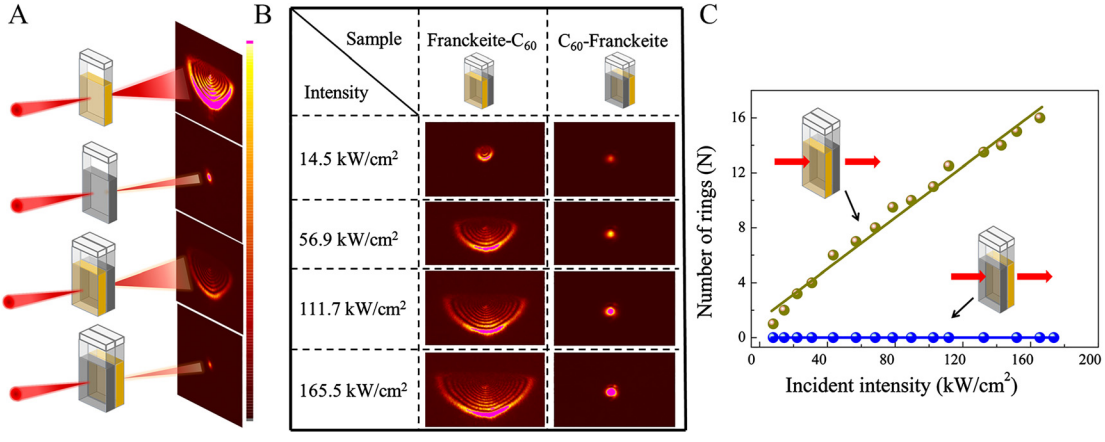

Figure 6: The experimental results obtained from the franckeite/C_{60}-based nonlinear photonic diode, and the phenomenon of unidirectional diffraction rings excitations.
(A) spatial self-phase modulation (SSPM) experimental device diagrams, the excitation structure from top to bottom are franckeite, C_{60}, franckeite-C_{60}, C_{60}-franckeite, respectively. It can be seen that only the franckeite and franckeite-C_{60} structures excite the diffraction ring. (B) The transmittance patterns of Gaussian beam through the forward and reverse bias structures under different light intensity. (C) The detailed changes in transmission characteristics of the two structures.

Gaussian beam evolves into a diffraction ring). It was found that the diffraction ring passes through C_{60} dispersion with a decrease intensity and an unchange number of rings (Figure 6A). However, when the laser passes through the reverse bias (C_{60}-franckeite), the light intensity is significantly reduced when it first passes through C_{60}, which will lower than the excitation threshold of the nonlinear characteristic of franckeite. Therefore, only a second decrease in light intensity will occur without a diffraction ring generation when franckeite is passed later, that is, the reverse light blocking of the photonic diode is implemented (diffraction rings are not generated and the light intensity is significantly reduced).

Under the same excitation light intensity, the transmittance patterns of Gaussian beam through the forward and reverse bias structures are shown in Figure 6B, and the diffraction ring can be excited under the franckeite-C_{60} structure, whereas the Gaussian beam still can be obtained under the C_{60}-franckeite structure. The detailed changes in transmission characteristics of the nonlinear photonic diode based on franckeite and C_{60} are shown in Figure 6C. It is clearly seen that the proposed franckeite/C_{60} hybrid structure can realize irreversible propagation of light, and the ring number can be modulated by the light intensity, which can be used as nonlinear photonic diodes.

5 Conclusions

In summary, we prepared layered franckeite by LPE method, and studied its nonlinear optical characteristics through Z-scan and SSPM experiments. We have obtained the nonlinear absorption coefficient of about -1.95×10^{-4} m/W, lower saturable intensity ~0.18 kW/cm^2, and large modulation depth of 9.4% of layered franckeite at near infrared spectral range. Ultrafast carrier dynamics characteristic with hundred picoseconds makes franckeite have the potential to contribute to the ultrafast optoelectronic devices. Combined the nonlinear optical characteristics of franckeite with the OL characteristics of C_{60}, the passive photonic diodes have been realized to achieve nonreciprocal transmission of light. By adjusting the nonlinear parameters, the nonreciprocal characteristics of the passive photonic diode can be tuned. Particularly, the low-threshold SA response, outstanding optical Kerr effect and ultrafast response of franckeite may provide some novel nonlinear optical application in the infrared regime. To meet the needs of low power consumption and high performance, franckeite with low nonlinear response threshold is an important candidate for ultrafast optoelectronic devices.

Acknowledgments: This work was supported in part by the National Natural Science Foundation of China under Grant 61775056, 61805076, 61975055, in part by Joint Equipment Pre-Research Foundation of the Ministry of Education of China under 6141A02033404 and in part by Natural Science Foundation of Hunan Province under Grant 2017JJ1013, 2019JJ50080.

Author contribution: All the authors have accepted responsibility for the entire content of this submitted manuscript and approved submission.

Research funding: This work was supported in part by the National Natural Science Foundation of China under Grant 61775056, 61805076, 61975055, in part by Joint Equipment Pre-Research Foundation of the Ministry of Education of China under 6141A02033404 and in part by Natural Science Foundation of Hunan Province under Grant 2017JJ1013, 2019JJ50080.

Conflict of interest statement: The authors declare no conflicts of interest regarding this article.

References

[1] H. Rydberg, M. Dion, N. Jacobson, et al., "Van der waals density functional for layered structures," *Phys. Rev. Lett.*, vol. 91, p. 126402, 2003.

[2] A. K. Geim and I. V. Grigorieva, "Van der Waals heterostructures," *Nature*, vol. 499, pp. 419–425, 2013.

[3] K. S. Novoselov, A. Mishchenko, A. Carvalho, and A. H. Castro Neto, "2D materials and van der Waals heterostructures," *Science*, vol. 353, p. aac9439, 2016.

[4] P. W. M. Blom, V. D. Mihailetchi, L. J. A. Koster, and D. E. Markov, "Device physics of polymer: fullerene bulk heterojunction solar cells," *Adv. Mater.*, vol. 19, pp. 1551–1566, 2007.

[5] J. H. Heo, S. H. Im, J. H. Noh, et al., "Efficient inorganic–organic hybrid heterojunction solar cells containing perovskite compound and polymeric hole conductors," *Nat. Photonics*, vol. 7, pp. 486–491, 2013.

[6] J. Low, J. Yu, M. Jaroniec, S. Wageh, and A. A. Al-Ghamdi, "Heterojunction photocatalysts," *Adv. Mater.*, vol. 29, p. 1601694, 2017.

[7] H. Wang, L. Zhang, Z. Chen, et al., "Semiconductor heterojunction photocatalysts: design, construction, and photocatalytic performances," *Chem. Soc. Rev.*, vol. 43, pp. 5234–5244, 2014.

[8] Q. Guo, M. Zhang, Z. Xue, et al., "Deterministic assembly of flexible Si/Ge nanoribbons via edge-cutting transfer and printing for van der Waals heterojunctions," *Small*, vol. 11, pp. 4140–4148, 2015.

[9] S. Masubuchi, M. Morimoto, S. Morikawa, et al., "Autonomous robotic searching and assembly of two-dimensional crystals to build van der Waals superlattices," *Nat. Commun.*, vol. 9, p. 1413, 2018.

[10] J. E. Padilha, A. Fazzio, and A. J. R. Da Silva, "Van der Waals heterostructure of phosphorene and graphene: tuning the Schottky barrier and doping by electrostatic gating," *Phys. Rev. Lett.*, vol. 114, p. 66803, 2015.

[11] R. Ribeiro-Palau, C. Zhang, K. Watanabe, T. Taniguchi, J. Hone, and C. R. Dean, "Twistable electronics with dynamically rotatable heterostructures," *Science*, vol. 361, pp. 690–693, 2018.
[12] L. Britnell, R. V. Gorbachev, R. Jalil, et al., "Field-effect tunneling transistor based on vertical graphene heterostructures," *Science*, vol. 335, pp. 947–951, 2012.
[13] T. Song, X. Cai, M. W. Y. Tu, et al., "Giant tunneling magnetoresistance in spin-filter van der Waals heterostructures," *Science*, vol. 360, pp. 1214–1218, 2018.
[14] F. Withers, O. Del Pozo-Zamudio, A. Mishchenko, et al., "Light-emitting diodes by band-structure engineering in van der Waals heterostructures," *Nat. Mater.*, vol. 14, pp. 301–306, 2015.
[15] Y. K. Ryu, R. Frisenda, and A. Castellanos-Gomez, "Superlattices based on van der Waals 2D materials," *Chem. Commun.*, vol. 55, pp. 11498–11510, 2019.
[16] Y. Niu, J. Villalva, R. Frisenda, et al., "Mechanical and liquid phase exfoliation of cylindrite: a natural van der Waals superlattice with intrinsic magnetic interactions," *2D Mater.*, vol. 6, p. 035023, 2019.
[17] R. A. W. Dryfe, "2D transition metal chalcogenides and van der Waals heterostructures: fundamental aspects of their electrochemistry," *Curr. Opin. Electrochem.*, vol. 13, pp. 119–124, 2019.
[18] J. Li, X. Yang, Y. Liu, et al., "General synthesis of two-dimensional van der Waals heterostructure arrays," *Nature*, vol. 579, pp. 368–374, 2020.
[19] M. Velický, P. S. Toth, A. M. Rakowski, et al., "Exfoliation of natural van der Waals heterostructures to a single unit cell thickness," *Nat. Commun.*, vol. 8, p. 14410, 2017.
[20] A. J. Molina-Mendoza, E. Giovanelli, W. S. Paz, et al., "Franckeite as a naturally occurring van der Waals heterostructure," *Nat. Commun.*, vol. 8, p. 14409, 2017.
[21] J. Li, K. Yang, l. Du, et al.., "Nonlinear optical response in natural van der Waals heterostructures," *Adv. Opt. Mater.*, vol. 2000382, pp. 1–9, 2020.
[22] R. Frisenda, G. Sanchez-Santolino, N. Papadopoulos, et al., "Symmetry breakdown in franckeite: spontaneous strain, rippling, and interlayer Moiré," *Nano Lett.*, vol. 20, pp. 1141–1147, 2020.
[23] P. Gant, F. Ghasemi, D. Maeso, et al., "Optical contrast and refractive index of natural van der Waals heterostructure nanosheets of franckeite," *Beilstein J. Nanotechnol.*, vol. 8, pp. 2357–2362, 2017.
[24] S. Gan, Y. Zhao, X. Dai, and Y. Xiang, "Sensitivity enhancement of surface plasmon resonance sensors with 2D franckeite nanosheets," *Results Phys.*, vol. 13, p. 101320, 2019.
[25] D. Steinberg, A. S. M. V. Oré, J. D. Zapata, E. A. Thoroh de Souza, and C. J. S. De Matos, "Third harmonic generation in mechanically exfoliated franckeite," in *Latin America Optics and Photonics Conference*, 2018.
[26] A. E. Willner, S. Khaleghi, M. R. Chitgarha, and O. F. Yilmaz, "All-optical signal processing," *J. Light. Technol.*, vol. 32, pp. 660–680, 2014.
[27] F. D. M. Haldane and S. Raghu, "Possible realization of directional optical waveguides in photonic crystals with broken time-reversal symmetry," *Phys. Rev. Lett.*, vol. 100, pp. 1–4, 2008.
[28] X. S. Lin, W. Q. Wu, H. Zhou, K. F. Zhou, and S. Lan, "Enhancement of unidirectional transmission through the coupling of nonlinear photonic crystal defects," *Opt. Express*, vol. 14, p. 2429, 2006.
[29] Y. Shoji, T. Mizumoto, H. Yokoi, I. W. Hsieh, and R. M. Osgood, "Magneto-optical isolator with silicon waveguides fabricated by direct bonding," *Appl. Phys. Lett.*, vol. 92, p. 071117, 2008.
[30] J. Hwang, M. H. Song, B. Park, et al., "Electro-tunable optical diode based on photonic bandgap liquid-crystal heterojunctions," *Nat. Mater.*, vol. 4, pp. 383–387, 2005.
[31] B. Anand, R. Podila, K. Lingam, et al., "Optical diode action from axially asymmetric nonlinearity in an all-carbon solid-state device," *Nano Lett.*, vol. 13, pp. 5771–5776, 2013.
[32] L. Wu, W. Huang, Y. Wang, et al., "2D tellurium based high-performance all-optical nonlinear photonic devices," *Adv. Funct. Mater.*, vol. 29, pp. 1–9, 2019.
[33] X. Yang, X. Hu, H. Yang, and Q. Gong, "Ultracompact all-optical logic gates based on nonlinear plasmonic nanocavities," *Nanophotonics*, vol. 6, pp. 365–376, 2017.
[34] J. Tang, F. Zhang, F. Zhou, X. Tang, X. Dai, and S. B. Lu, "Broadband nonlinear optical response in GeSe nanoplates and its applications in all-optical diode," *Nanophotonics*, vol. 9, pp. 2007–2015, 2020.
[35] Z. Sun, A. Martinez, and F. Wang, "Optical modulators with 2D layered materials," *Nat. Photonics*, vol. 10, pp. 227–238, 2016.
[36] K. F. Mak and J. Shan, "Photonics and optoelectronics of 2D semiconductor transition metal dichalcogenides," *Nat. Photonics*, vol. 10, pp. 216–226, 2016.
[37] S. C. Dhanabalan, J. S. Ponraj, H. Zhang, and Q. Bao, "Present perspectives of broadband photodetectors based on nanobelts, nanoribbons, nanosheets and the emerging 2D materials," *Nanoscale*, vol. 8, pp. 6410–6434, 2016.
[38] V. Nicolosi, M. Chhowalla, M. G. Kanatzidis, M. S. Strano, and J. N. Coleman, "Liquid exfoliation of layered materials," *Science*, vol. 340, p. 1226419, 2013.
[39] T. D. Krauss and F. W. Wise, "Raman-scattering study of exciton-phonon coupling in PbS nanocrystals," *Phys. Rev. B Condens. Matter Mater. Phys.*, vol. 55, pp. 9860–9865, 1997.
[40] T. D. Krauss and F. W. Wise, "Coherent acoustic phonons in a semiconductor quantum dot," *Phys. Rev. Lett.*, vol. 79, pp. 5102–5105, 1997.
[41] A. J. Smith, P. E. Meek, and W. Y. Liang, "Raman scattering studies of SnS_2 and $SnSe_2$ the effect of polytypism on the band structure of SnS Raman scattering studies of SnS, and $SnSe_2$," *J. Phys. C Solid State Phys.*, vol. 10, p. 1, 1997.
[42] C. Wang, K. Tang, Q. Y. Aa, and Y. Qian, "Raman scattering, far infrared spectrum and photoluminescence of SnS_2 nanocrystallites," *Chem. Phys. Lett.*, vol. 357, pp. 371–375, 2002.
[43] S. V. Ovsyannikov, V. V. Shchennikov, A. Cantarero, A. Y. Cros, and A. N. Titov, "Raman spectra of $(PbS)_{1.18}(TiS_2)_2$ misfit compound," *Mater. Sci. Eng. A*, vol. 462, pp. 422–427, 2007.
[44] G. D. Smith, S. Firth, R. J. H. Clark, and M. Cardona, "First- and second-order Raman spectra of galena (PbS)," *J. Appl. Phys.*, vol. 92, pp. 4375–4380, 2002.
[45] M. Sheik-Bahae, A. A. Said, T. H. Wei, D. J. Hagan, and E. W. Van Stryland, "Sensitive measurement of optical nonlinearities using a single beam," *IEEE J. Quantum Electron.*, vol. 26, pp. 760–769, 1990.
[46] H. Zhang, S. Virally, Q. Bao, et al., "Z-scan measurement of the nonlinear refractive index of graphene," *Opt. Lett.*, vol. 37, p. 1856, 2012.

[47] M. Liu, X. Yin, E. Ulin-avila, et al., "A graphene-based broadband optical modulator," *Nature*, vol. 474, pp. 64–67, 2011.
[48] Q. Wu, S. Chen, Y. Wang, et al., "MZI-based all-optical modulator using MXene $Ti_3C_2T_x$ (T = F, O, or OH) deposited microfiber," *Adv. Mater. Technol.*, vol. 4, p. 1800532, 2019.
[49] B. Guo, Q. L. Xiao, S. H. Wang, and H. Zhang, "2D layered materials: synthesis, nonlinear optical properties, and device applications," *Laser Photonics Rev*, vol. 13, pp. 1–46, 2019.
[50] M. Zhang, Q. Wu, F. Zhang, et al., "2D black phosphorus saturable absorbers for ultrafast photonics," *Adv. Opt. Mater.*, vol. 1800224, pp. 1–18, 2019.
[51] R. L. Sutherland, D. G. Mclean, and S. Kirkpatrick, *Handbook of Nonlinear Optics*, New York, Marcel Dekker, 2003.
[52] J. Li, Z. L. Zhang, J. Yi, et al., "Broadband spatial self-phase modulation and ultrafast response of MXene $Ti_3C_2T_x$ (T = O, OH or F)," *Nanophotonics*, vol. aop, pp. 1–10, 2020.
[53] L. Wu, Y. Dong, J. Zhao, et al., "Kerr nonlinearity in 2D graphdiyne for passive photonic diodes," *Adv. Mater.*, vol. 31, p. 1807981, 2019.
[54] L. Wu, Z. Xie, L. Lu, et al., "Few-layer tin sulfide: a promising black-phosphorus-analogue 2D material with exceptionally large nonlinear optical response, high stability, and applications in all-optical switching and wavelength conversion," *Adv. Opt. Mater.*, vol. 6, pp. 1–10, 2018.